

Accepted Manuscript

Correlation between the magnetic and thermoelectric properties in $Mg_{2-x}Mn_xSi$

Chungman Kim, Soohyun Kim, Yang-Ki Hong, Min-Wook Oh, Myung-Hwa Jung



PII: S0925-8388(16)32473-2

DOI: [10.1016/j.jallcom.2016.08.095](https://doi.org/10.1016/j.jallcom.2016.08.095)

Reference: JALCOM 38597

To appear in: *Journal of Alloys and Compounds*

Received Date: 10 May 2016

Revised Date: 14 July 2016

Accepted Date: 12 August 2016

Please cite this article as: C. Kim, S. Kim, Y.-K. Hong, M.-W. Oh, M.-H. Jung, Correlation between the magnetic and thermoelectric properties in $Mg_{2-x}Mn_xSi$, *Journal of Alloys and Compounds* (2016), doi: 10.1016/j.jallcom.2016.08.095.

This is a PDF file of an unedited manuscript that has been accepted for publication. As a service to our customers we are providing this early version of the manuscript. The manuscript will undergo copyediting, typesetting, and review of the resulting proof before it is published in its final form. Please note that during the production process errors may be discovered which could affect the content, and all legal disclaimers that apply to the journal pertain.

Correlation between the magnetic and thermoelectric properties in $\text{Mg}_{2-x}\text{Mn}_x\text{Si}$

Chungman Kim^{a,b}, Soohyun Kim^c, Yang-Ki Hong^d, Min-Wook Oh^e, Myung-Hwa Jung^{a,*}

^aDepartment of Physics, Sogang University, Seoul 04107, South Korea

^bResearch Institute for Basic Science, Sogang University, Seoul 04107, South Korea

^cCenter for Electronic Materials, Korea Institute of Science and Technology, Seoul 02792, South Korea

^dDepartment of Electrical and Computer Engineering, University of Alabama, Alabama 35487, USA

^eDepartment of Advanced Materials Engineering, Hanbat National University, Daejeon 34158, South Korea

* Corresponding author. Tel.: +82 2 705 8828

E-mail address: mhjung@sogang.ac.kr

Abstract

Single crystals of $\text{Mg}_{2-x}\text{Mn}_x\text{Si}$ ($x = 0, 0.1, 0.2, 0.3,$ and 0.4) were prepared using a vertical Bridgman method. The formation of desired materials was confirmed using single-crystal and powder X-ray diffraction. The thermoelectric and magnetic properties were investigated for various Mn contents in the temperature range between 2 and 300 K and in magnetic fields up to 70 kOe. For various x values, $\text{Mg}_{2-x}\text{Mn}_x\text{Si}$ with $x = 0.2$ possesses the highest figure of merit. The experimental results revealed that the substitutional Mn atoms exhibit mixed valences of +3 (majority) and +2, giving rise to dramatic changes of carrier density and magnetic interaction. At the same time, the Seebeck coefficient and magnetic susceptibility show a sudden change at the same temperature. These results imply that the thermoelectric properties are correlated with the magnetic properties in the $\text{Mg}_{2-x}\text{Mn}_x\text{Si}$ crystals.

Keywords : Thermoelectric materials, Magnetic properties, Mg_2Si , Mn substitution

1. Introduction

The thermoelectric efficiency is estimated by the figure of merit, ZT , defined by $ZT = (S^2\sigma/\kappa)T$, where S is the Seebeck coefficient, σ is the electrical conductivity, κ is the thermal conductivity, and T is the absolute temperature. For high performance of thermoelectric materials, it is important to have high Seebeck coefficient, high electrical conductivity, and low thermal conductivity at desired temperature range. However, it is difficult to achieve the above conditions simultaneously because these physical parameters are competing with each other. In commercial applications, the thermoelectric materials can be divided into three groups, depending on the temperature range of operation: [1-5] one is near-room-temperature region based on Bi–Te alloys, the other is intermediate-temperature region from 500 to 900 K based on Pb–Te alloys, and another is high-temperature region above 900 K based on silicide alloys.

Mg_2Si is well known as a semiconductor with an indirect band gap of 0.78 eV and a thermoelectric material with high energy conversion efficiency at high temperatures [6-12]. This material satisfies the requirement for commercial thermoelectric applications being environmental-friendly, and the elements are composed of light metals, abundant in the earth and cost effective. The Seebeck coefficient of pure Mg_2Si reaches up to $S = -500 \mu\text{V/K}$ but only $ZT = 0.1$ [10,13], and thereby there have been many efforts to improve the thermoelectric properties with proper dopants into Mg_2Si . Appropriate doping enhances the thermoelectric performance because the impurity states strongly influences the electronic transport properties. Most of studies have been focused on polycrystalline Mg_2Si samples prepared by spark plasma sintering [6], hot pressing [7], and solid solution [8]. Doping elements used for improving thermoelectric performance in Mg_2Si are Al, Bi, Sb, Pb, and Ge [6-11]. In comparison with the polycrystalline samples, there have been a few reports on single crystals of Mg_2Si series. Recently, Akasaka *et al.* have reported that the ZT values are 0.65 at 840 K and 0.1 at 566 K for Bi- and Ag-doped Mg_2Si single crystals, respectively, synthesized by the vertical Bridgman growth method [12]. The Bridgman method is useful to prevent the evaporation of Mg near the melting point of Mg_2Si .

While the thermoelectric performance can be significantly improved with proper dopants, the thermoelectric properties at low temperatures even in pure Mg_2Si crystals have not been carefully reported so far. In this study, we focus on the correlation between the magnetic and thermoelectric properties by Mn substitution in Mg_2Si , which is more efficient at lower temperature, so that the low-temperature studies with single crystals are important. The Mn atoms in $\text{Mg}_{2-x}\text{Mn}_x\text{Si}$ have five 3d electrons, which are magnetic in nature. In the energy scheme, the half-filled 3d bands can not only affect the density of states at the Fermi level, which governs the electrical properties, but also change the spin states, which may be energetically more favorable. The main aim in this study is to find a correlation between the thermoelectric and magnetic properties by magnetic impurity doping at low temperatures. With increasing the Mn composition, both electrical conductivity and magnetization data are monotonically enhanced. It can be explained by an enhancement in the density of states, as the band overlap increases. Furthermore, we observe a sudden slope change in the Seebeck coefficient curve around 85 K, where the magnetic susceptibility shows a broad peak. This result proposes that the thermoelectric properties can be correlated with the magnetic properties via magnetic impurity doped bands.

2. Experimental procedure

Single crystals of $\text{Mg}_{2-x}\text{Mn}_x\text{Si}$ ($x = 0, 0.1, 0.2, 0.3, 0.4$) were grown by vertical Bridgman method. The starting elements of bulk Mg (99.9%), granular Si (99.999%), and bulk Mn (99.9%) were put into a Mo crucible with the stoichiometric amounts and the crucible was sealed by using arc melting under Ar atmosphere. Then, the crucible was heated up to 1100°C for two days in a high-vacuum (2.0×10^{-6} Torr) Bridgman chamber with tungsten heater, and was cooled down to room temperature over one week as rotating at 5 rpm.

The crystal structure was analyzed by X-ray diffraction using a Rigaku DMAX 2500 diffractometer with $\text{CuK}\alpha$ radiation ($\lambda = 1.5406 \text{ \AA}$). The grown crystals were well cleaved and were cut into approximately $3 \times 3 \times 7 \text{ mm}^3$ rectangular bar samples for the thermal and electronic transport measurements. Seebeck coefficient and thermal conductivity measurements were performed with a

thermoelectric option in a Quantum Design physical property measurement system (PPMS). The Seebeck coefficient, thermal conductivity, and electrical conductivity were measured by conventional four-probe method, using silver paint or epoxy for the electrical contact. The error of each measurement was within 2%. The electronic transport properties were measured in a Gifford-McMahon (GM) refrigerator, and the magnetic properties were measured in a superconducting quantum measurement system-vibrating sample magnetometer (SQUID-VSM). The magnetic field was applied along the cleaved surface of the crystals.

3. Results and discussion

Figs 1(a) and (b) show the single-crystal and powder X-ray diffraction (XRD) patterns of $\text{Mg}_{2-x}\text{Mn}_x\text{Si}$ ($x = 0, 0.1, 0.2, 0.3, \text{ and } 0.4$) samples. The single-crystal XRD data were taken from a shiny and flat surface. The single-crystal diffraction peaks are well labeled with the (111) indices of the face-centered-cubic (fcc) CaF_2 -type structure, where Si atoms occupy the corners and face-centered positions of the unit cell and Mg atoms occupy eight tetrahedral sites $(\pm\frac{1}{4}, \pm\frac{1}{4}, \pm\frac{1}{4})a^3$. The high intensity of (111) peaks is known to stem from a cleavage characteristic of the anti-fluorite type structure of Mg_2Si [14]. In order to check the existence of secondary phases, we measured powder XRD patterns, which were obtained by grinding the single crystals. As shown in Fig. 1(b), the peak intensity of (111) is reduced and the (220) peak is enhanced. This result is consistent with the previous report that the area of the (111) plane decreases due to smaller grains [14]. The main diffraction peaks are indexed with the reported structure of Mg_2Si [12], but a small amount of impurity phases arising from Mo_xSi_y is detected around $2\theta = 43^\circ$. The peak position of impurity phases is marked with arrows and the peak intensity of impurity phases is as small as 3%. The Mo-related impurity comes from the contamination of Mo crucible during the fabrication processes. Except those Mo-related impurity peaks, all the peak positions shift to higher angle. This indicates that the lattice parameter decreases with increasing the Mn substitution. The obtained lattice parameter is $a = 6.374 \text{ \AA}$ for $x = 0$, then monotonically decreases with x , reaching $a = 6.359 \text{ \AA}$ for $x = 0.4$, as listed in Table 1. It can be simply explained by the smaller ionic size of Mn^{3+} substituted for Mg^{2+} [15], which will be discussed later.

The temperature dependence of electrical conductivity (σ) for $\text{Mg}_{2-x}\text{Mn}_x\text{Si}$ ($x = 0.1, 0.2, 0.3, 0.4$) is shown in Fig. 2(a). The electrical conductivity data were taken on the shiny surface parallel to the current direction. The electrical conductivity tends to decrease with increasing x (except for $x = 0.2$). Above 85 K, the conductivity for $x = 0.2$ becomes higher than others. The maximum conductivity is obtained to be 117 S/cm at 180 K in $x = 0.2$. The decrease of electrical conductivity with x can be attributed to the Mn impurity scattering which reduces the carrier mobility and/or the decrease of Mg occupancy which leads to the decrease of carrier density [16]. In order to check the respective contribution, we performed the Hall measurements to determine the carrier density and carrier mobility. The results are summarized in Table 1. All the samples exhibit n -type charge carriers. For pure Mg_2Si ($x = 0$), the n -type carriers are well known to originate from the formation of positively charged Mg ions at interstitial sites, regardless of the chemical composition in crystal growth [16]. On increasing Mn contents of the samples (except for $x = 0.2$ at low temperature), the n -type carrier density increases and the carrier mobility decreases more significantly. This result indicates that the carrier mobility, not carrier density, governs the electrical conduction where the carrier transport is strongly affected by Mn impurities. In $\text{Mg}_{2-x}\text{Mn}_x\text{Si}$ materials, when both Mg and Mn ions have the same valence state ($2+$), no significant change of carrier density can be expected. It may change the concentration of Mg vacancy that is considered as a major defect in the material. The Mg vacancy, i.e. the decrease of Mg occupancy, acts as an acceptor to reduce the electron carrier density because the Fermi level moves from the bottom of conduction band down into the band gap [14,17,18]. Thereby, the electrical transport in $\text{Mg}_{2-x}\text{Mn}_x\text{Si}$ cannot be explained by considering the same valence states of Mn and Mg. For this reason, we construct different Mn ionic state of Mn^{3+} ($3d^4$). When Mn^{3+} is substituted at the Mg^{2+} sites, electron carrier doping is significant to enhance the n -type carrier density. This scenario elucidates the increase of carrier density with the increase in Mn content and well agrees with the decrease of lattice parameter because the ionic radius of Mn^{3+} is smaller than that of Mn^{2+} [15]. These results support the presence of Mn^{3+} as a major valence state of Mn. On the other hand, the carrier mobility significantly decreases with the increase of Mn content. There are at least two strong candidates for the origin. One is the Mn impurity scattering, which reduces the carrier

mobility. The other is more electron-electron scattering for higher x with larger carrier density.

The temperature dependence of Seebeck coefficient (S) for $\text{Mg}_{2-x}\text{Mn}_x\text{Si}$ ($x = 0.1, 0.2, 0.3, 0.4$) is shown in Fig. 2(b). Except the low temperature regime for $x = 0.1$ (inset of Fig. 2(b)), all the samples exhibit negative Seebeck coefficient. This reflects n -type charge carriers, which is consistent with the result observed in the Hall measurements. The n -type characteristic of Mg_2Si is explained by positively charged defect such as Mg at an interstitial site, that is Mg_i acting as a donor [16]. The absolute value of Seebeck coefficient tends to decrease with increasing x (except for $x = 0.1$). This tendency can be simply understood in a convenient way where the Seebeck coefficient is inversely proportional to the carrier density. As seen in Table 1, the carrier density monotonically increases as the Mn contents increase. In practice, the change of Seebeck coefficient with x is attributed not only to the carrier density but also to the difference in the carrier mobility and band structure. Here it should be noted that the absolute value of Seebeck coefficient appears to be the highest at $x = 0.2$, where the electrical conductivity is the highest. The Seebeck coefficient reaches a maximum of $-175 \mu\text{V/K}$ at 300 K in $x = 0.2$. While the absolute values of Seebeck coefficient are different for each sample, the temperature dependence reveals a similar behavior. On heating, the absolute Seebeck coefficient simply increases for all the samples, which is a typical behavior for a degenerate semiconductor because the Fermi level moves away from the edge of conduction band [19]. In Fig. 2(b), the Seebeck coefficient shows a small change in slope near 85 K, which is almost in the temperature range of the maximum structure of electrical conductivity. Although both Seebeck coefficient and Hall coefficient are negative, a zoom on the low-temperature data for $x = 0.1$ reveals positive Seebeck coefficient below 85 K (the inset of Fig. 2(b)). The positive sign yields the presence of p -type carriers in the low temperature region for $x = 0.1$, where the electrical conductivity shows a sudden rise at low temperature. This temperature dependence of both Seebeck coefficient and electrical conductivity is probably due to the competition and/or coexistence of electron and hole carriers.

The temperature dependence of thermal conductivity (κ) for $\text{Mg}_{2-x}\text{Mn}_x\text{Si}$ ($x = 0.1, 0.2, 0.3, 0.4$) is shown in Fig. 2(c). The measured thermal conductivity is composed of two different components:

electronic and phonon conductivities (κ_{el} and κ_{ph} , respectively). In convenient, the electronic thermal conductivity can be estimated by the Wiedemann-Franz relation [10,12,20,21], from which the obtained κ_{el} values are almost two order of magnitude smaller than the κ values. Thereby, the κ_{ph} component has a dominant role in the temperature dependence of total thermal conductivity. Although the variation of thermal conductivity with different x is complicated, the temperature dependence for all the samples shows similar behavior. With increasing temperatures, the thermal conductivity increases and then decreases above 85 K with the $1/T$ dependence, which is the typical behavior at high temperatures due to the strong phonon-phonon scattering (i.e. Umklapp process) [22].

We calculate the figure of merit $ZT = (S^2\sigma/\kappa)T$ for $\text{Mg}_{2-x}\text{Mn}_x\text{Si}$ ($x = 0.1, 0.2, 0.3, 0.4$), which is plotted in Fig. 2(d). The ZT values for all the samples monotonically increase as the temperature increases, and the ZT values for $x = 0.2$ and 0.3 are much higher than those for $x = 0.1$ and 0.4 . The calculated ZT value reaches 0.004 at 300 K for the $x = 0.2$ sample. We may compare this value to those obtained in other doped Mg_2Si systems. For instance, M. Akasaka *et al.* reported a maximum $ZT = 0.1$ at room temperature for Bi-doped Mg_2Si , which is much higher than ours because they obtained much higher electrical conductivity. It is usual that the electrical conductivity is sensitive to the doping elements. Although the lower electrical conductivity in $\text{Mg}_{2-x}\text{Mn}_x\text{Si}$ gives rise to the lower ZT , we would point out that the Mn substitution into Mg_2Si enormously changes the carrier density and carrier mobility. This infers that the ZT value may be improved if the carrier density and mobility is optimized by the substitution contents and synthesis process.

Mg_2Si is a non-magnetic material, but it becomes magnetic when Mn is substituted for Mg. The Mn ion seems to be a source of magnetism in $\text{Mg}_{2-x}\text{Mn}_x\text{Si}$. We measured the magnetization as a function of magnetic field and temperature for $\text{Mg}_{2-x}\text{Mn}_x\text{Si}$ ($x = 0.1, 0.2, 0.3, 0.4$), which was performed with the external magnetic field applied parallel to the crystal plane. The results are depicted in Fig. 3. As seen in Figs. 3(a) and 3(b), the magnetization increases in magnitude with increasing the Mn composition. The pure Mg_2Si ($x = 0$) exhibits diamagnetic property, while the others show linear dependence at 300 K and S-shaped curves at 50 K. The S-curves are observed

below 85 K, where the magnetization divided by magnetic field (M/H) in Figs. 3(c)-(f) displays a broad peak. At first glance, the temperature dependence seems to be antiferromagnetic with a Néel temperature $T_N = 85$ K. Although there is a separation of zero-field-cooled (ZFC) and field-cooled (FC) data below 85 K, it is insufficient to insist that $\text{Mg}_{2-x}\text{Mn}_x\text{Si}$ is antiferromagnetic. Here, we suggest the correlation between the magnetic and thermoelectric properties in $\text{Mg}_{2-x}\text{Mn}_x\text{Si}$. Even though we did not observe any appreciable change in M/H for the amount of Mn contents, a definite change occurs for Mn substitution. The pure Mg_2Si shows no dependence of temperature and magnetic field in the magnetic properties. With increasing x , the absolute value of M/H increases, demonstrating that Mn is well substituted for Mg. The results can be explained by an enhancement in the density of states by doping the magnetic impurities of Mn. As aforementioned, the major valence state of Mn ions is trivalent, which is substituted for Mg^{2+} , so that the overlap of Mn(3d) impurity band with conduction band increases and the density of states at the Fermi level increases. Indeed, we observed the increase in n -type carrier density and the decrease in lattice parameter by substituting Mn for Mg, since the substitutional Mn^{3+} ions act as electron dopants and the ionic radius of Mn^{3+} is larger than that of Mg^{2+} , respectively. At the same time, the magnetization dramatically increases, suggesting that the magnetic interaction is driven by substituting Mn. When the M/H represents a broad peak around 85 K, the Seebeck coefficient is changed in slope at that temperature. This is the evidence on the correlation between the magnetic and thermoelectric properties. In addition, this temperature is close the temperature range where the electrical conductivity shows a small maximum and the thermal conductivity exhibits a peak structure. Thus, we can conclude that the electron dopants created by the Mn substitution play an important role in both magnetic and thermoelectric properties.

The low-temperature data can be interpreted on the basis of magnetothermoelectric effect observed in Bi_2Te_3 alloys [23]. They reported a crossover of the Seebeck coefficient from p - to n -type below 100 K, where the electrical transport displays unusual nonmetallic temperature dependence. Similar behavior is observed for $x = 0.1$ in $\text{Mg}_{2-x}\text{Mn}_x\text{Si}$. There is a crossover regime in the Seebeck coefficient from n - to p -type below 85 K, and simultaneously the electrical conductivity shows a

change in slope. In order to clearly address the role of Mn impurity band, we need to investigate more experiments such as magnetic circular dichroism and inelastic neutron scattering.

4. Conclusions

The electrical conductivity, Seebeck coefficient, thermal conductivity, and magnetic moments of $\text{Mg}_{2-x}\text{Mn}_x\text{Si}$ alloys have been measured with single crystals for different x ($= 0.1, 0.2, 0.3, 0.4$) in the temperature range between 2 and 300 K and in magnetic fields up to 70 kOe. Despite low figure of merit ZT , we would emphasize that the electrical conductivity can be improved by the Mn substitution. The substitutional Mn allows to dramatically not only change the carrier density and carrier mobility but also induce the magnetic moment from nonmagnetic Mg_2Si ($x = 0$) sample. The X-ray diffraction and electrical transport data support the presence of Mn^{3+} as a major valence state of Mn, which acts as electron dopants and induces the magnetic interaction. We observe a sudden slope change in the Seebeck coefficient around 85 K, where the magnetization shows a broad peak. These results propose the correlation between magnetic and thermoelectric properties in $\text{Mg}_{2-x}\text{Mn}_x\text{Si}$.

Acknowledgment

This work was supported by the National Research Foundation of Korea (NRF) grant funded by the Korea government (MEST) (No. 2014R1A2A1A1105401).

References

- [1] P. Pierrat, A. Dauscher, B. Lenoir, R. Martin-Lopez, H. Scherrer, Preparation of the $\text{Bi}_8\text{Sb}_{32}\text{Te}_{60}$ solid solution by mechanical alloying, *J. Mater. Sci.* 32 (1997) 3653-3657.
- [2] H. C. Kim, T. S. Oh, D. -B. Hyun, Thermoelectric properties of the *p*-type $\text{Bi}_2\text{Te}_3\text{-Sb}_2\text{Te}_3\text{-Sb}_2\text{Se}_3$ alloys fabricated by mechanical alloying and hot pressing, *J. Phys. Chem. Solids* 61 (2000) 743-749.
- [3] N. Bouad, M. -C. Record, J. -C. Tedenac, R. -M. Marin-Ayral, Mechanical alloying of a thermoelectric alloy: $\text{Pb}_{0.65}\text{Sn}_{0.35}\text{Te}$, *J. Solid State Chem.* 177 (2004) 221-226.
- [4] S. W. Kim, M. K. Cho, Y. Mishima, D. C. Choi, High temperature thermoelectric properties of *p*- and *n*-type $\beta\text{-FeSi}_2$ with some dopants, *Intermetallics* 11 (2003) 399-405.
- [5] A. Heinrich, H. Griessmann, G. Behr, K. Ivanenko, J. Schumann, H. Vinzelberg, Thermoelectric properties $\beta\text{-FeSi}_2$ single crystals and polycrystalline $\beta\text{-FeSi}_{2+x}$ thin films, *Thin Solid Films* 381 (2001) 287-295.
- [6] J. Tani, H. Kido, Thermoelectric properties of Sb-doped Mg_2Si semiconductors, *Intermetallics* 15 (2007) 1202-1207.
- [7] A. U. Khan, N. Vlachos, Th. Kyratsi, High thermoelectric figure of merit of $\text{Mg}_2\text{Si}_{0.55}\text{Sn}_{0.4}\text{Ge}_{0.05}$ materials doped with Bi and Sb, *Scripta Mater.* 69 (2013) 606-609.
- [8] Y. Noda, H. Kon, Y. Furukawa, N. Otsuka, I. A. Nishida, K. Masumoto, Preparation and thermoelectric properties of $\text{Mg}_2\text{Si}_{1-x}\text{Ge}_x$ ($x = 0.0\sim 0.4$) solid solution semiconductors, *Mater. Trans., JIM* 33 (1992) 845-850.
- [9] J. Tani, H. Kido, Thermoelectric properties of Al-doped $\text{Mg}_2\text{Si}_{1-x}\text{Sn}_x$ ($x \leq 0.1$), *J. Alloys Compd.* 466 (2008) 335-340.
- [10] S. Muthiah, J. Pulikkotil, A. K. Srivastava, A. Kumar, B. D. Pathak, A. Dhar, R. C. Budhani, Conducting grain boundaries enhancing thermoelectric performance in doped Mg_2Si , *App. Phys. Lett*

103 (2013) 053901.

[11] Y. Noda, H. Kon, Y. Furukawa, I. A. Nishida, K. Masumoto, Temperature dependence of thermoelectric properties of $\text{Mg}_2\text{Si}_{0.6}\text{Ge}_{0.4}$, Mater. Trans., JIM 33 (1992) 851-855.

[12] M. Akasaka, T. Iida, A. Matsumoto, K. Yamanaka, Y. Takanashi, T. Imai, N. Hamada, The thermoelectric properties of bulk crystalline *n*- and *p*-type Mg_2Si prepared by the vertical Bridgman method, J. Appl. Phys. 104 (2008) 013703.

[13] J. Tani, H. Kido, Thermoelectric properties of Bi-doped Mg_2Si semiconductors, Physica B 364 (2005) 218-224.

[14] M. Kubouchi, K. Hayashi, Y. Miyazaki, Quantitative analysis of interstitial Mg in Mg_2Si studied by single crystal X-ray diffraction, J. Alloys Compd. 617 (2014) 389-392.

[15] R. D. Shannon, Revised effective ionic radii and systematic studies of interatomic distances in halides and chalcogenides, Acta Crystallogr. A32 (1976) 751-767

[16] A. Kato, T. Yagi, N. Fukusako, First-principles studies of intrinsic point defects in magnesium silicide, J. Phys.: Condens. Matter 21 (2009) 205801.

[17] Y. Imai, A. Watanabe, M. Mukaida, Electronic structures of semiconducting alkaline-earth metal silicides, J. Alloys Compd. 358 (2003) 257-263.

[18] J. Tobola, S. Kaprzyk, H. Scherrer, Mg-vacancy-induced semiconducting properties in $\text{Mg}_2\text{Si}_{1-x}\text{Sb}_x$ from electronic structure calculations, J. Electron. Mater. 39 (2010) 2064-2069.

[19] H. J. Goldsmid, J. W. Sharp, Estimation of the thermal band gap of a semiconductor from Seebeck measurements, J. Electron. Mater. 28 (1999) 869-872.

[20] G. J. Snyder, E. S. Toberer, Complex thermoelectric materials, Nat. Mater. 7 (2008) 105-114.

[21] J. Zhao, Z. Liu, J. Reid, K. Takarabe, T. Iida, B. Wang, U. Yoshiya, J. S. Tse, Thermoelectric and electrical transport properties of Mg_2Si multi-doped with Sb, Al and Zn, J. Mater. Chem. A 3 (2015) 19774-19782

[22] N. W. Ashcroft, N. D. Mermin, Solid State Physics, Holt, Rinehart and Winston, New York, 1976, p. 501.

[23] Y. S. Hor, D. Qu, N. P. Ong, R. J. Cava, Low temperature magnetothermoelectric effect and magnetoresistance in Te vapor annealed Bi_2Te_3 , J. Phys.: Condens. Matter 22 (2010) 375801.

ACCEPTED MANUSCRIPT

Table 1. Lattice constant a , carrier density n , and carrier mobility μ measured at 300 K and 3 K in $\text{Mg}_{2-x}\text{Mn}_x\text{Si}$ for $x = 0, 0.1, 0.2, 0.3$, and 0.4 .

| x | a (Å) | 300 K | | 3 K | |
|-----|---------|-----------------------------------|-----------------------------------|-----------------------------------|-----------------------------------|
| | | n (10^{17} cm^{-3}) | μ (cm^2/Vs) | n (10^{17} cm^{-3}) | μ (cm^2/Vs) |
| 0 | 6.374 | 7.41 | 376 | 8.53 | 491 |
| 0.1 | 6.366 | 12.4 | 282 | 10.2 | 461 |
| 0.2 | 6.362 | 21.0 | 256 | 0.678 | 1107 |
| 0.3 | 6.359 | 104 | 25.2 | 73.6 | 10.2 |
| 0.4 | 6.359 | 111 | 1.74 | 32.9 | 0.537 |

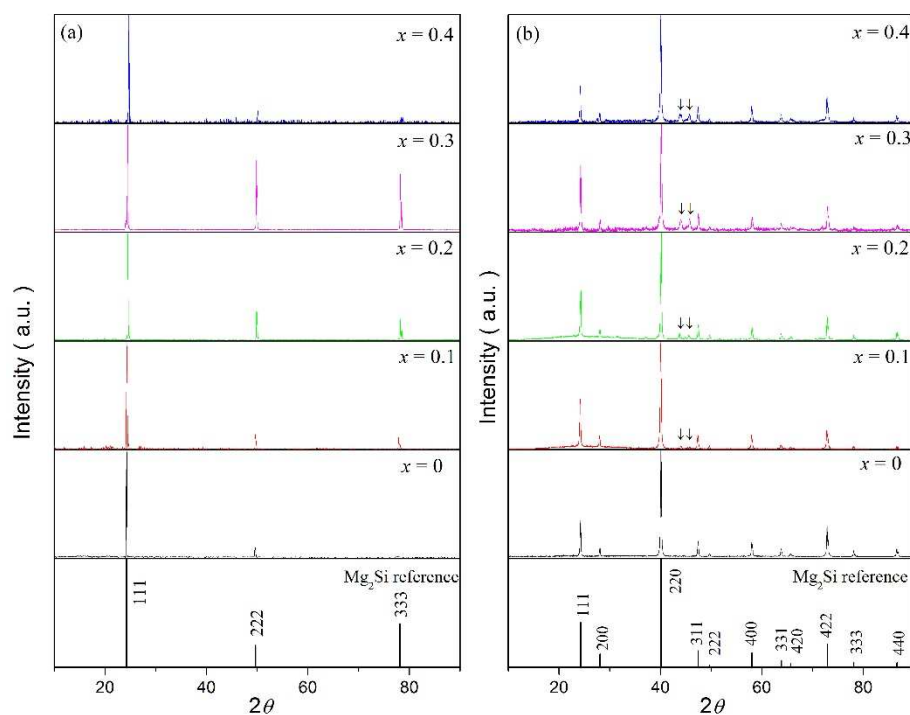


Fig. 1. (a) Single-crystal and (b) powder X-ray diffraction (XRD) patterns of $\text{Mg}_{2-x}\text{Mn}_x\text{Si}$ ($x = 0, 0.1, 0.2, 0.3, 0.4$). The reference data of Mg_2Si is plotted in the bottom panel.

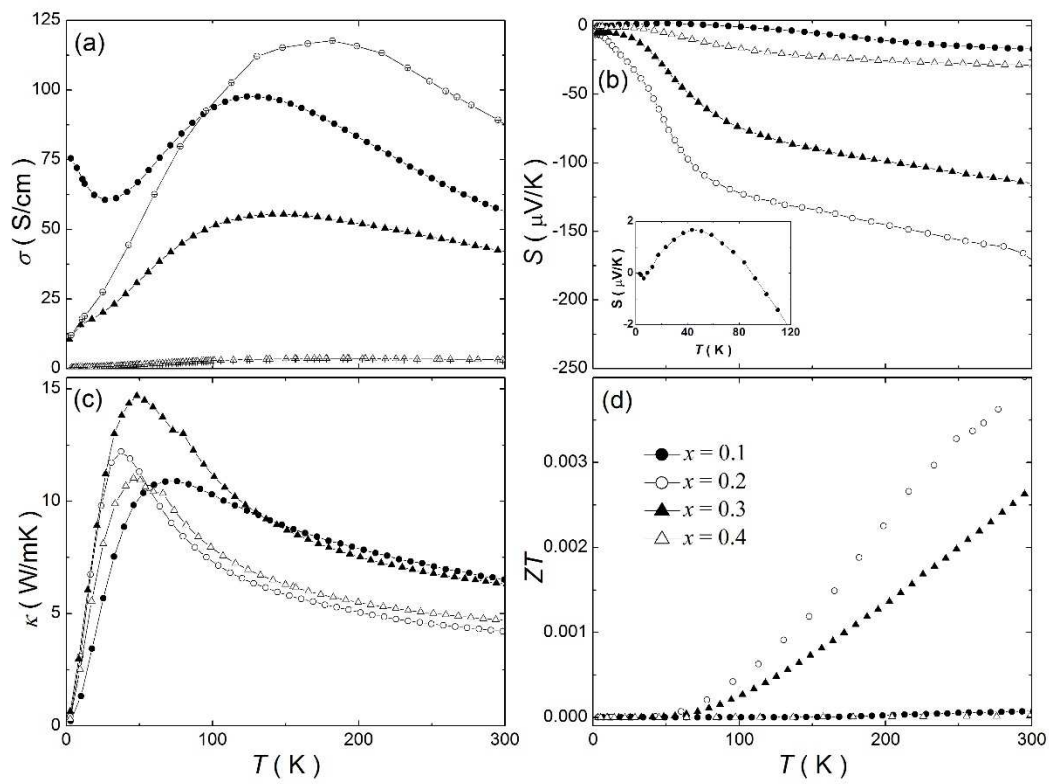


Fig. 2. Temperature dependence of (a) electrical conductivity σ , (b) Seebeck coefficient S , (c) thermal conductivity κ , and (d) figure of merits ZT obtained in $\text{Mg}_{2-x}\text{Mn}_x\text{Si}$ ($x = 0.1, 0.2, 0.3, 0.4$). The inset of Figs. 2(b) shows the low-temperature S data for $x = 0.1$.

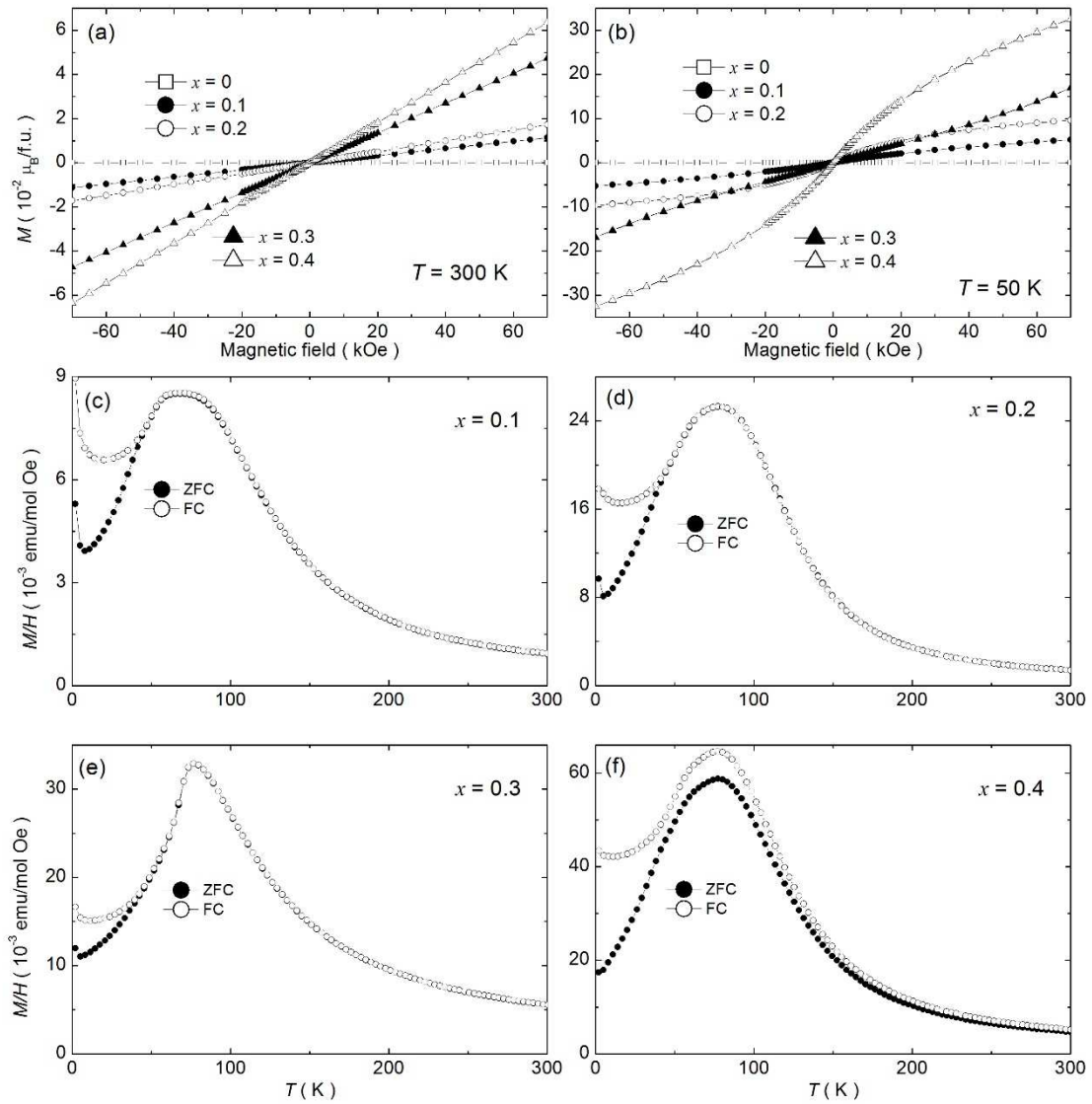


Fig. 3. Magnetic field dependence of magnetization M measured at (a) 300 K and (b) 50 K for $\text{Mg}_{2-x}\text{Mn}_x\text{Si}$ ($x = 0.1, 0.2, 0.3, 0.4$). Temperature dependence of magnetization divided by magnetic field (M/H) measured in 1 kOe for $x =$ (c) 0.1, (d) 0.2, (e) 0.3, and (f) 0.4. The closed and open circles represent zero-field-cooled (ZFC) and field-cooled (FC) data, respectively.

Highlights

- Single crystals of $\text{Mg}_{2-x}\text{Mn}_x\text{Si}$ were prepared by using a vertical Bridgman method.
- The thermoelectric performance was improved as doping Mn into Mg_2Si .
- The magnetic properties were enhanced with Mn dopants.
- The thermoelectric and magnetic properties were strongly correlated in $\text{Mg}_{2-x}\text{Mn}_x\text{Si}$.